

# Single-channel activity of L-type $\text{Ca}^{2+}$ channels reconstituted with the $\beta_{2c}$ subunit cloned from the rat heart

Yasuhiro Kamada<sup>a,b</sup>, Yoichi Yamada<sup>a</sup>, Michiaki Yamakage<sup>b,\*</sup>, Masato Nagashima<sup>a</sup>,  
Masaaki Tsutsuura<sup>a</sup>, Takeshi Kobayashi<sup>a</sup>, Sumihiko Seki<sup>a</sup>,  
Akiyoshi Namiki<sup>b</sup>, Noritsugu Tohse<sup>a</sup>

<sup>a</sup>Department of Cellular Physiology and Signal Transduction, Sapporo Medical University School of Medicine, Sapporo, Hokkaido 060-8543, Japan

<sup>b</sup>Department of Anesthesiology, Sapporo Medical University School of Medicine, South 1, West 16, Chuo, Sapporo, Hokkaido 060-8543, Japan

Received 7 August 2003; received in revised form 5 January 2004; accepted 21 January 2004

## Abstract

We recently cloned the  $\beta_{2c}$  subunit of the L-type  $\text{Ca}^{2+}$  channel as a functional type of  $\beta$  subunit from the rat heart. In order to clarify the contribution of the  $\beta_{2c}$  subunit to native  $\text{Ca}^{2+}$  channel function, we investigated the single-channel properties of  $\text{Ca}^{2+}$  channels reconstituted with  $\beta_{2a}$  or  $\beta_{2c}$  subunits and compared them with the properties of native channels. In contrast to the  $\text{Ca}^{2+}$  channel with  $\beta_{2a}$  subunit, long-lasting closings were dominant in the  $\text{Ca}^{2+}$  channel with  $\beta_{2c}$  subunit and the native channel. The ensemble-averaged current of the cells with  $\beta_{2c}$  subunits was comparable to that of the native cardiomyocytes. Many high  $P_o$  sweeps (mode 2) were observed in the cells with  $\beta_{2a}$  subunits, while only a few high  $P_o$  sweeps were observed in the cells with  $\beta_{2c}$  subunits and the native cells. These findings suggest that the  $\beta_{2c}$  subunit is one of the functional  $\beta$  subunits in the rat heart.

© 2004 Elsevier B.V. All rights reserved.

**Keywords:** L-type  $\text{Ca}^{2+}$  channel;  $\beta_{2c}$  Subunit; Single-channel analysis; Modal gating behavior

## 1. Introduction

L-type  $\text{Ca}^{2+}$  channels play an important role in excitation–contraction coupling of the heart (Bers, 2002).  $\text{Ca}^{2+}$  entry through L-type  $\text{Ca}^{2+}$  channels contributes to the action potential plateau and triggers  $\text{Ca}^{2+}$  release from the sarcoplasmic reticulum. The cardiac L-type  $\text{Ca}^{2+}$  channel is composed of four distinct subunits, i.e., the pore-forming subunit  $\alpha_{1c}$  and auxiliary subunits  $\beta$  and  $\alpha_2\delta$  (Catterall, 2000; Perez-Reyes and Schneider, 1995). The  $\alpha_{1c}$  subunit is sufficient to produce functional  $\text{Ca}^{2+}$  channel molecules, but its expression level and kinetics are regulated by the auxiliary subunits (Catterall, 2000; Birnbaumer et al., 1998). Among them, the  $\beta$  subunit has been shown to play a central role in functional aspects of the  $\text{Ca}^{2+}$  channel (Birnbaumer et al., 1998; Lacerda et al., 1991). The  $\beta$  subunit affects activation

and inactivation kinetics and is essential for proper transportation of the  $\text{Ca}^{2+}$  channel to the membrane (Birnbaumer et al., 1998; Lacerda et al., 1991). To date, four distinct  $\beta$  subunits ( $\beta_1$ ,  $\beta_2$ ,  $\beta_3$ , and  $\beta_4$ ), and their splice variants have been cloned and expressed in different tissues and regions (Perez-Reyes and Schneider, 1995; Birnbaumer et al., 1998; Hofmann et al., 1994). The  $\beta_{2a}$  subunit has been reported to express in the rat heart (Perez-Reyes et al., 1992). Thus, in cardiac myocytes,  $\text{Ca}^{2+}$  channels are thought to be mainly associated with the  $\beta_{2a}$  subunit. However, in a recent study, polymerase chain reaction (PCR) product corresponding to the rat  $\beta_{2a}$  subunit was not detected in the rabbit heart using the rat  $\beta_{2a}$  specific primers (Qin et al., 1998). Moreover, inactivation rates of the  $\text{Ca}^{2+}$  current ( $I_{Ca}$ ) from native cardiac  $\text{Ca}^{2+}$  channels were found to be faster than those from L-type  $\text{Ca}^{2+}$  channels containing the rat  $\beta_{2a}$  subunit in a heterologous expression system (Wei et al., 2002). Therefore, it is not clear whether the  $\beta_{2a}$  subunit actually functions in the rat heart.

Recently, we have cloned a splice variant of the  $\beta_2$  subunit from the rat heart, which we named rat  $\beta_{2c}$  subunit

\* Corresponding author. Tel.: +81-11-611-2111x3568; fax: +81-11-631-9683.

E-mail address: [yamakage@sapmed.ac.jp](mailto:yamakage@sapmed.ac.jp) (M. Yamakage).

(Yamada et al., 2001). The deduced amino acid sequence of the  $\beta_{2c}$  subunit was different from that of the rat  $\beta_{2a}$  subunit only in the N-terminal region. Northern blot analysis revealed that the rat  $\beta_{2c}$  subunit is abundantly present in the rat heart and brain. On the other hand, the  $\beta_{2a}$  subunit was detected in the rat brain but not in the rat heart. L-type  $\text{Ca}^{2+}$  currents reconstituted with  $\beta_{2c}$  subunits showed inactivation rates comparable with those recorded from native rat cardiomyocytes, although the current with the  $\beta_{2a}$  subunit showed slow inactivation. These observations strongly suggest that the  $\beta_{2c}$  subunit is one of the  $\beta$  subunits functioning in the heart.

The difference in inactivation rates suggests that  $\beta$  subunits affect the gating properties of  $\text{Ca}^{2+}$  channels. To investigate the roles of  $\beta$  subunits in the gating properties of  $\text{Ca}^{2+}$  channels, we performed single-channel recordings of reconstituted L-type  $\text{Ca}^{2+}$  channels with the  $\beta_{2a}$  subunit or the  $\beta_{2c}$  subunit and native rat cardiac  $\text{Ca}^{2+}$  channels.

In the present study, the single-channel properties of the  $\text{Ca}^{2+}$  channel with  $\beta_{2c}$  subunit were indistinguishable from those of the native channel and different from the

$\text{Ca}^{2+}$  channel with the  $\beta_{2a}$  subunit. These findings support our previous study that the  $\beta_{2c}$  subunit is one of the functional  $\beta$  subunits in the rat heart.

## 2. Materials and methods

### 2.1. Expression of L-type $\text{Ca}^{2+}$ channels in COS-7 cells

$\beta_{2a}$  subunits cloned from the rat brain and  $\beta_{2c}$  subunits cloned from the rat heart were expressed in COS-7 cells together with  $\alpha_{1c}$  and  $\alpha_{2\delta}$  subunits cloned from the rat heart as described previously (Yamada et al., 2001). In brief, COS-7 cells were transiently transfected with 1  $\mu\text{g}$  of pIRES- $\alpha_{2\delta}$ -hrGFP together with pIRES- $\alpha_{1c}$ - $\beta_{2a}$  or pIRES- $\alpha_{1c}$ - $\beta_{2c}$  using Effectene™ transfection reagent (Qiagen, Valencia, CA, USA) according to the manufacturer's instructions. Cells were subsequently maintained on collagen-coated coverslip fragments in Dulbecco's modified Eagle's medium supplemented with 10% fetal calf serum, 30  $\mu\text{g}/\text{ml}$  streptomycin, and 30 U/ml penicillin and assayed after 24–96 h.

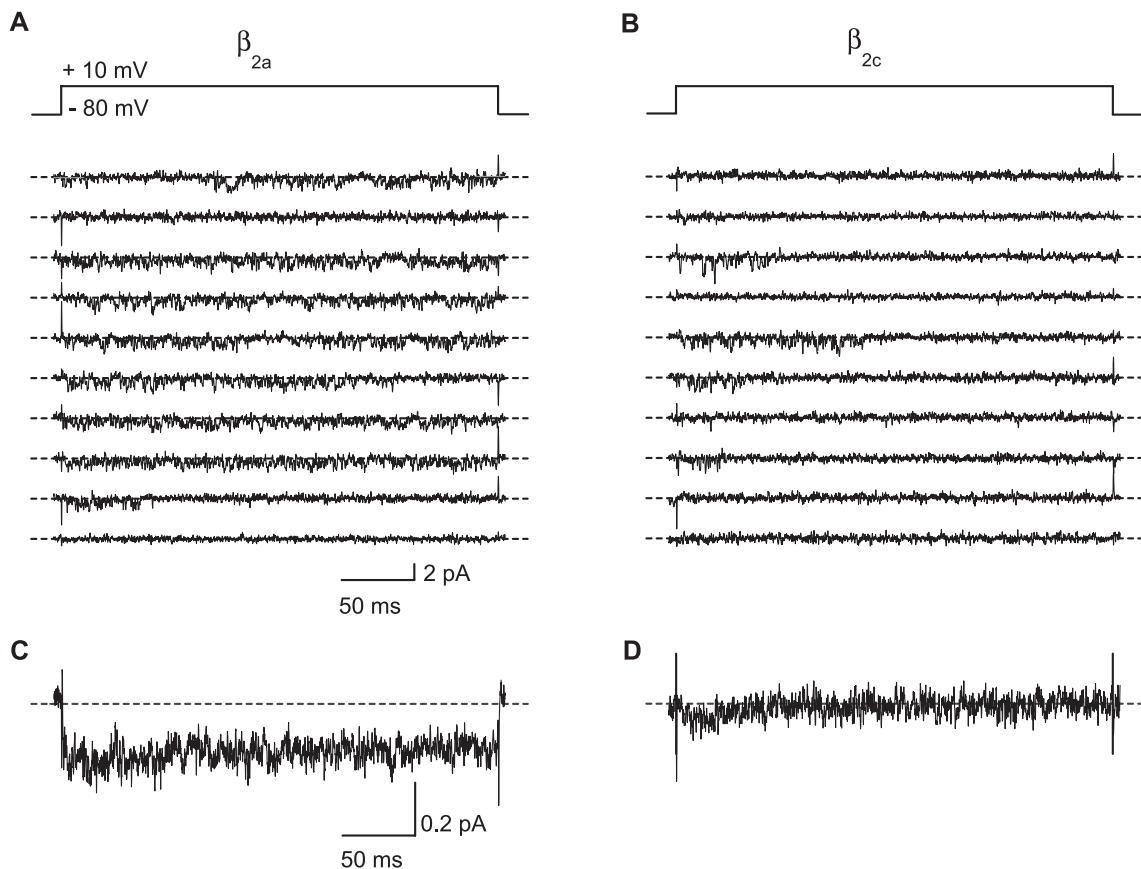


Fig. 1. Representative current sweeps of single  $\text{Ca}^{2+}$  channel activity in COS-7 cell transfected with  $\beta_{2a}$  subunits (A), COS-7 cell transfected with  $\beta_{2c}$  subunits (B) elicited by consecutive depolarizing pulses to +10 mV (from a holding potential of -80 mV, 300 ms) every 5 s in a cell-attached patch configuration. The pulse protocol is shown above the set of tracings. Linear leak and capacity currents have been subtracted. Downward deflection of the tracing reflects channel opening. The lower panel shows the ensemble-averaged currents with 132 sweeps (C), from 141 sweeps with  $\beta_{2c}$  subunits (D). The horizontal dotted line indicates the zero current level.

## 2.2. Preparation of single cardiac myocytes

Single ventricular myocytes were enzymatically isolated from the ventricles of rat hearts as described previously (Tohse, 1990). In brief, hearts were removed from rats anesthetized with pentobarbital and perfused in a Langendorff apparatus with 0.02–0.04% collagenase (Wako, Osaka, Japan) dissolved in nominally  $\text{Ca}^{2+}$ -free Tyrode solution. After 30 min of digestion, the left ventricle of each heart was rinsed with Kraftbrühe (KB) solution (Isenberg and Klockner, 1982), cut into small pieces, and shaken to separate cells. The composition of the nominally  $\text{Ca}^{2+}$ -free Tyrode solution was (in mM): NaCl 143, KCl 5.4,  $\text{MgCl}_2$  0.5,  $\text{NaH}_2\text{PO}_4$  0.33, glucose 5.5, and HEPES 5 (pH 7.4, titrated by 1 N NaOH). The KB solution was composed of (in mM): KCl 40, KOH 70,  $\text{NaH}_2\text{PO}_4$  20, *L*-glutamic acid 50, taurine 20,  $\text{MgCl}_2$  3, EGTA 1, glucose 10, and HEPES 10 (pH 7.4, titrated by 1 N KOH). The cell suspension in the KB solution was stored in a refrigerator at 4 °C for later use.

## 2.3. Electrophysiological measurement and data analysis

Coverslip fragments with attached cells or isolated cardiac myocytes were continuously perfused on the stage of an inverted microscope. Transfected cells were identified by the expression of hrGFP. Cell-attached patch clamp

recordings were made using pipettes with resistance of 5–10 M $\Omega$ . Pipettes were pulled from capillary tubes in a two-step process and coated with insulating varnish. The cells were perfused with normal Tyrode solution at 37 °C. After gigaseal formation, the perfusate was changed to an external depolarizing solution containing 150 mM  $\text{K}^+$ . The membrane potential of the cells should be approximately 0 mV in this solution. Activities of single  $\text{Ca}^{2+}$  channels were measured as unitary  $\text{Ba}^{2+}$  current ( $I_{\text{Ba}}$ ) through a single channel by the use of a pipette solution containing 110 mM  $\text{Ba}^{2+}$ . The composition of the normal Tyrode solution was (in mM): NaCl 143, KCl 5.4,  $\text{CaCl}_2$  1.8,  $\text{MgCl}_2$  0.5,  $\text{NaH}_2\text{PO}_4$  0.33, glucose 5.5, and HEPES 5 (pH 7.4, titrated by 1 N NaOH). The external depolarizing solution contained (in mM): KCl 140,  $\text{MgCl}_2$  0.5, glucose 5.5, EGTA 10, and HEPES 5 (pH 7.4, titrated by 1 N KOH). The pipette solution was composed of (in mM):  $\text{BaCl}_2$  110, and HEPES 5 (pH 7.4, titrated by 1 N Tris). In a part of the experiments, 1  $\mu\text{M}$  of Bay K 8644 (1,4-dihydro-2,6-dimethyl-5-nitro-4-[2-(trifluoromethyl) phenyl] pyridine-3-carboxylic acid methyl ester), a  $\text{Ca}^{2+}$  channel activator, was added to the pipette solution to enhance the channel activities for detailed analyses.

Depolarization test pulses to +10 mV from a holding potential of –80 mV elicited single-channel currents. The test pulses were applied to cells at a rate of 0.2 Hz for a period of 300 or 1000 ms. To obtain current–

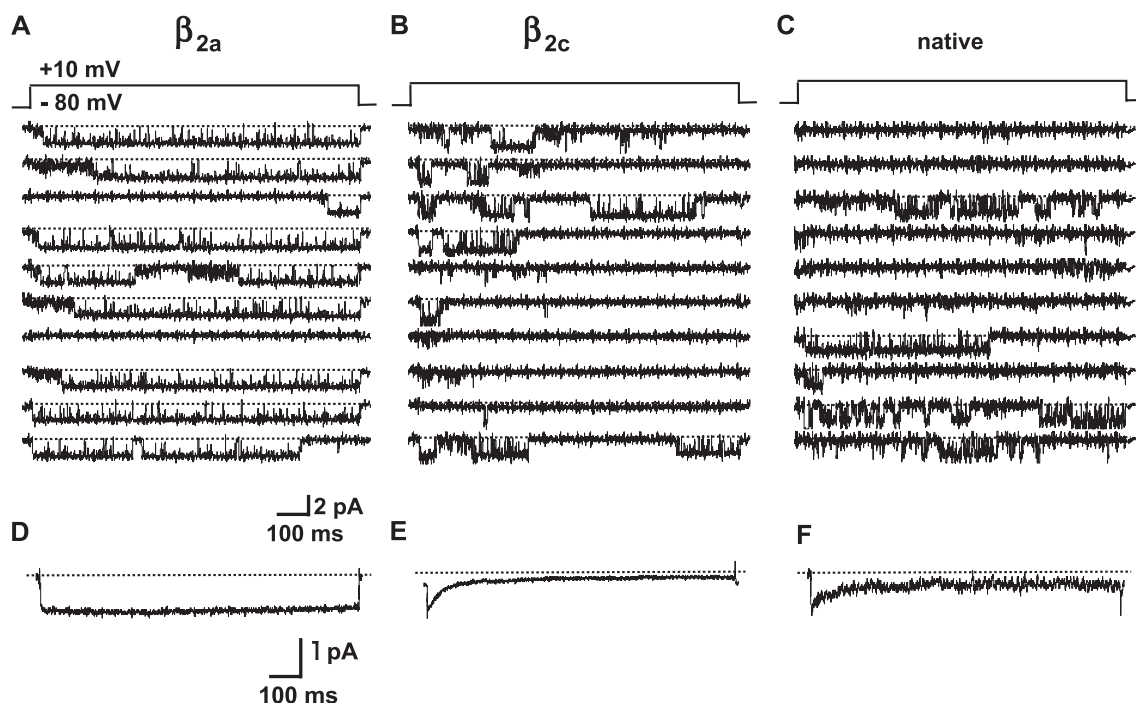


Fig. 2. Representative current sweeps of single  $\text{Ca}^{2+}$  channel activity in COS-7 cells transfected with  $\beta_{2a}$  subunits (A), COS-7 cells transfected with  $\beta_{2c}$  subunits (B), and native rat cardiac myocytes (C) elicited by consecutive depolarizing pulses to +10 mV (from a holding potential of –80 mV, 1000 ms) every 5 s in a cell-attached patch configuration. The pulse protocol is shown above the set of tracings. Linear leak and capacity currents have been subtracted. Downward deflection of the tracing reflects channel opening. The lower panel shows the ensemble-averaged currents from 598 sweeps from three cells with  $\beta_{2a}$  subunits (D), from 975 sweeps from five cells with  $\beta_{2c}$  subunits (E), and from 915 sweeps from four native rat cardiac myocytes (F). The horizontal dotted line indicates the zero current level.

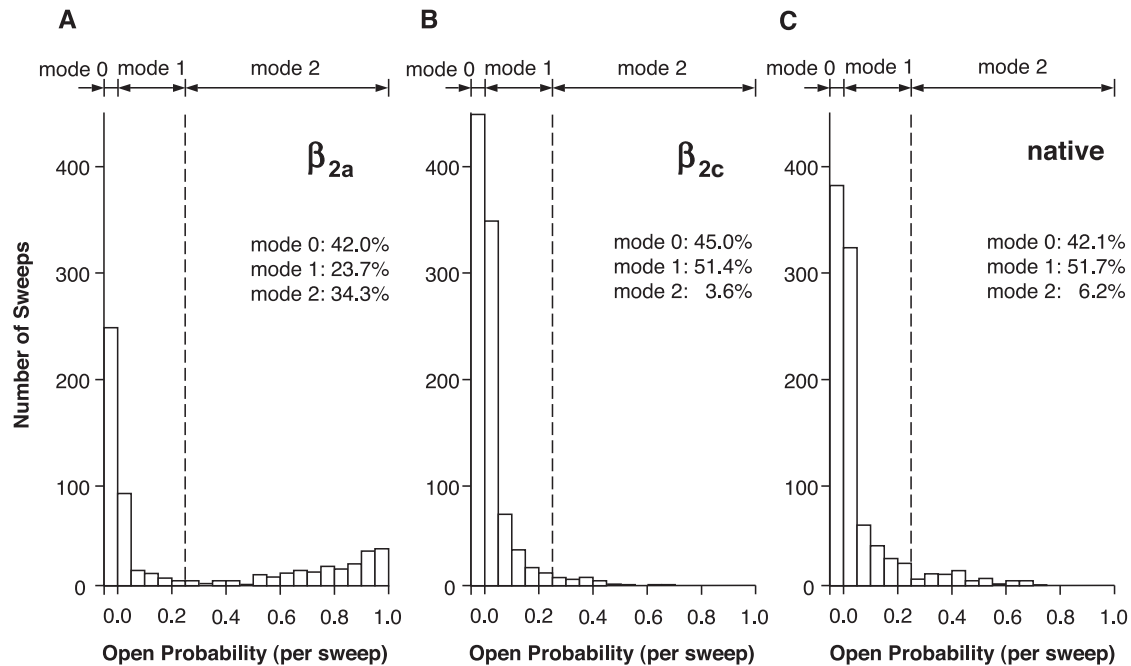


Fig. 3. Histograms of the distribution of open probability for each sweep in cells with  $\beta_{2a}$  subunits (A), cells with  $\beta_{2c}$  subunits (B), and native cells (C) compiled from 598 sweeps from three cells with  $\beta_{2a}$  subunits, from 975 sweeps from five cells with  $\beta_{2c}$  subunits, and from 915 sweeps from four native cells, respectively. Mode 0 indicates an open probability of 0, mode 1 indicates low open probability ( $0 < P_o \leq 0.25$ ), and mode 2 indicates an open probability  $> 0.25$ . The bin width was 0.05 units of probability.

voltage relations, depolarizing pulses to  $-30$ ,  $-20$ ,  $-10$ ,  $0$ ,  $+10$ , and  $+20$  mV were applied. Analysis and voltage protocols were performed with the use of an Axopatch 1D amplifier/Digidata 1322A interface (Clampex software, pCLAMP 8.2, Axon Instruments, Union City, CA, USA). Current signals were filtered at 2 kHz by a low-pass filter and digitized at 10 kHz. Single-channel data were analyzed using pCLAMP 8.2 software (Axon Instruments).

All values are presented as means  $\pm$  S.E.M. Slope conductance was analyzed by the method of least squares. Open time and closed time histograms were fitted by the maximum likelihood method. Statistical analyses were performed by one-way analysis of variance (ANOVA) and Fisher's a post hoc test.  $P < 0.05$  was considered significant.

### 3. Results

#### 3.1. Single-channel activities

Fig. 1 shows representative consecutive sweeps of single-channel activities from COS-7 cells transfected with pIRES- $\alpha_{1c}$ - $\beta_{2a}$  (Fig. 1A) or pIRES- $\alpha_{1c}$ - $\beta_{2c}$  (Fig. 1B). In most sweeps of the cells with  $\beta_{2a}$  subunits, very short openings were observed during the entire depolarizing pulse. On the other hand, in sweeps of the cells with  $\beta_{2c}$  subunits, the channel opening tended to occur at the pulse beginning. Ensemble-

averaged current of the cells with  $\beta_{2a}$  subunits (Fig. 1C) remained large at the pulse end, but ensemble-averaged current of the cells with  $\beta_{2c}$  subunits (Fig. 1D) declined immediately. Similar observations were obtained in different patches ( $n = 4$  for  $\beta_{2a}$  subunits,  $n = 3$  for  $\beta_{2c}$  subunits). This result agrees with our previous study that the whole-cell current of the cells with  $\beta_{2c}$  subunits inactivated faster than

Table 1

Time constants and proportions of open time distributions

	Fast component		Slow component	
	Time constant (ms)	Proportion	Time constant (ms)	Proportion
<i>All sweeps</i>				
$\beta_{2a}$	$3.89 \pm 0.23$	$0.32 \pm 0.09$	$14.78 \pm 2.75$	$0.67 \pm 0.09$
$\beta_{2c}$	$1.76 \pm 0.15^*$	$0.62 \pm 0.01^*$	$12.34 \pm 2.34$	$0.38 \pm 0.01^*$
Native	$2.67 \pm 0.31^*$	$0.79 \pm 0.10^*$	$11.97 \pm 1.04$	$0.21 \pm 0.10^*$
<i>Low <math>P_o</math> sweeps (mode 1)</i>				
$\beta_{2a}$	$1.90 \pm 0.55$	$0.78 \pm 0.12$	$14.87 \pm 4.10$	$0.21 \pm 0.12$
$\beta_{2c}$	$1.67 \pm 0.17$	$0.75 \pm 0.04$	$11.67 \pm 1.50$	$0.25 \pm 0.04$
Native	$2.24 \pm 0.19$	$0.86 \pm 0.07$	$12.01 \pm 1.78$	$0.14 \pm 0.07$
<i>High <math>P_o</math> sweeps (mode 2)</i>				
$\beta_{2a}$	$5.71 \pm 0.72$	$0.48 \pm 0.13$	$15.60 \pm 3.05$	$0.50 \pm 0.13$
$\beta_{2c}$	$2.81 \pm 0.54$	$0.55 \pm 0.17$	$17.27 \pm 3.24$	$0.36 \pm 0.15$
Native	$3.99 \pm 0.83$	$0.50 \pm 0.25$	$13.23 \pm 1.48$	$0.48 \pm 0.26$

Values are means  $\pm$  S.E.M. Three, four and five experiments were carried out for cells with  $\beta_{2a}$  subunits, cells with  $\beta_{2c}$  subunits, and native cells, respectively. Low  $P_o$  sweeps (mode 1),  $0 < \text{open probability} \leq 0.25$ ; high  $P_o$  sweeps (mode 2), open probability  $> 0.25$ .

\*Significant vs.  $\beta_{2a}$  group ( $P < 0.05$ ).

that of the cells with  $\beta_{2c}$  subunits. (Yamada et al., 2001). However, because success rate of stable patch recording was very low, we cannot perform more statistical analysis.

Bay K 8644 (1  $\mu$ M), a  $\text{Ca}^{2+}$  channel activator, was added to the pipette solution to enhance the channel activities because basal single-channel activities were too low to analyze. As we thought that inactivation kinetics were very important to analyze in further detail, long depolarizing test pulses of 1000 ms duration were applied. Unitary  $I_{\text{Ba}}$  with Bay K 8644 was recorded from COS-7 cells transfected with  $\beta_{2a}$  subunits or  $\beta_{2c}$  subunits and isolated rat cardiomyocytes. The unit amplitudes of the unitary currents were almost the same in all cell types. The slope conductances of the channels were  $31.6 \pm 1.6$  pS (cells with  $\beta_{2a}$ ,  $n=6$ ),  $32.0 \pm 1.2$  pS (cells with  $\beta_{2c}$ ,  $n=5$ ) and  $31.8 \pm 0.6$  pS (native cells,  $n=5$ ). Single-channel activities recorded by this method were represented in Fig. 2. As shown in Fig. 2A, long-lasting openings of the  $\text{Ca}^{2+}$  channel were frequently observed in the cells with  $\beta_{2a}$  subunits, and open probability ( $P_o$ ) was high in many sweeps. Although some long-lasting openings were also observed in the cells with  $\beta_{2c}$  subunits (Fig. 2B), the frequency of long-lasting open-

ing was lower than that in the cells with  $\beta_{2a}$  subunits. Long-lasting closings were more dominant in the cells with  $\beta_{2c}$  subunits than in the cells with  $\beta_{2a}$  subunits. Single-channel activity recorded similarly from native cardiomyocytes (Fig. 2C) resembled that of the cells with  $\beta_{2c}$  subunits. Ensemble-averaged inward currents of both the cells with  $\beta_{2c}$  subunits and the native cells declined exponentially during test pulses, but there was little decline in that of the cells with  $\beta_{2a}$  subunits (Fig. 2D–F).

### 3.2. Variations in open probability

Fig. 3 shows sweep-to-sweep variations in openings of the  $\text{Ca}^{2+}$  channels.  $P_o$  plotted on the abscissa is the open probability of each sweep. These histograms were compiled from all current sweeps of all examined cells for each experimental condition. We defined three modes of gating for further analysis as follows (Tohse et al., 1992). Null sweeps (mode 0) were sweeps in which no channel activity was found, low  $P_o$  sweeps (mode 1) were those in which low  $P_o$  ( $0 < P_o \leq 0.25$ ) was found, and high  $P_o$  sweeps (mode 2) were those with  $P_o > 0.25$ , consisting mainly of

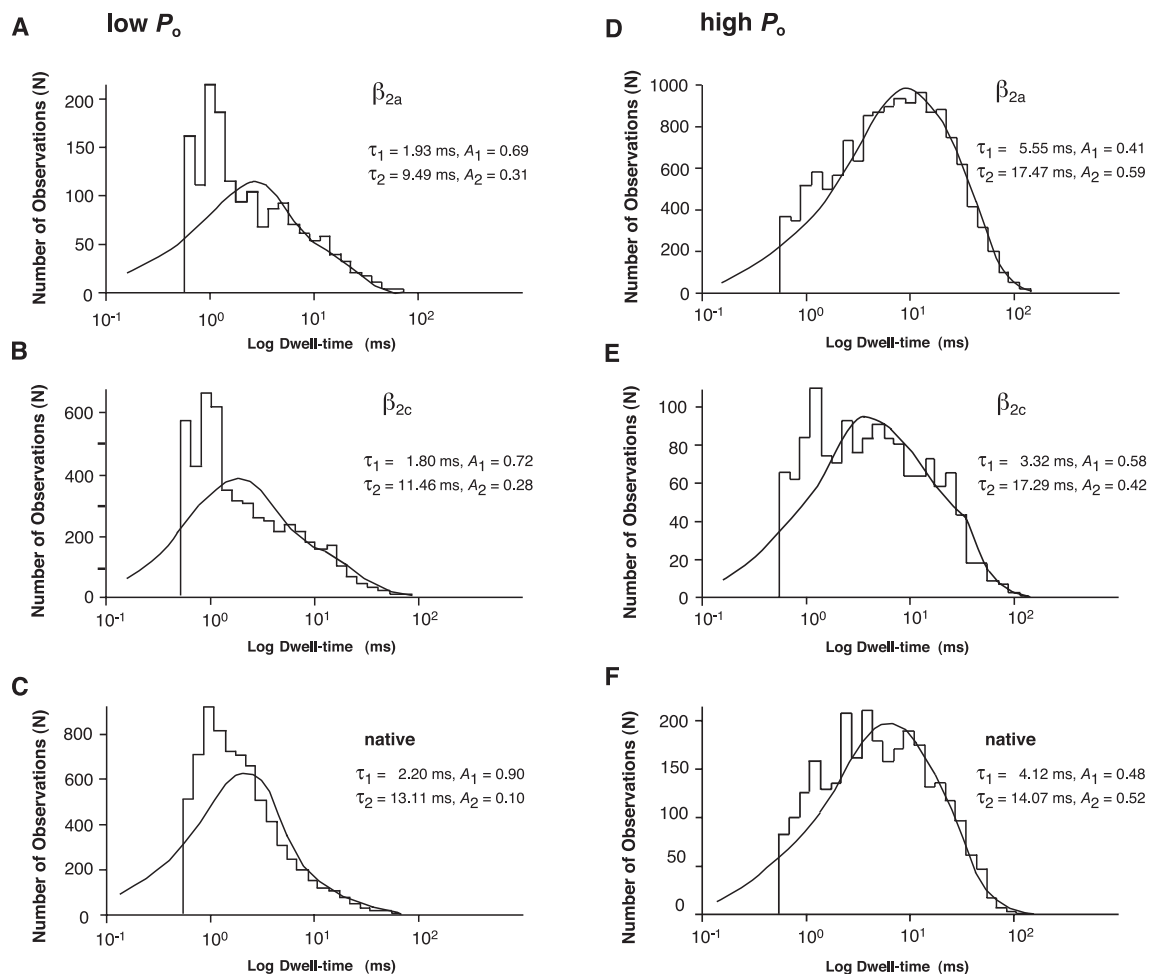


Fig. 4. Open time histograms compiled from separated low  $P_o$  sweeps (A, B, C) and high  $P_o$  sweeps (D, E, F). The upper panel (A, D) shows histograms from cells with  $\beta_{2a}$  subunits, the middle panel (B, E) shows histograms from cells with  $\beta_{2c}$  subunits, and the lower panel (C, F) shows histograms from native cells.

long-lasting openings. Fig. 3A shows the distribution of values of  $P_o$  from COS-7 cells transfected with  $\beta_{2a}$  subunits. The histogram shows a bimodal distribution with high  $P_o$  sweeps accounting for 34.3% of all sweeps. On the other hand, in the cells with  $\beta_{2c}$  subunits (Fig. 3B), the proportion of high  $P_o$  sweeps was very low, accounting for only 3.6% of all sweeps. Only a few high  $P_o$  sweeps were observed in the native cells, as shown in the histogram (Fig. 3C). In native cardiac myocytes, high  $P_o$  sweeps accounting for 6.2% of all sweeps. These data indicate that the frequency of long-lasting openings (mode 2) was much lower in the cells with  $\beta_{2c}$  subunit and the native cells than in the cells with  $\beta_{2a}$  subunit.

### 3.3. Open time distributions

The open time distributions were analyzed. In all cases, open time histograms could be fitted to the sum of two exponential functions. The distribution of open times of cells with  $\beta_{2a}$  subunits was different from the distributions of open times of cells with  $\beta_{2c}$  subunits and native cells. The parameters for the open time distribution of each cell type used for statistical analysis are shown in Table 1. Although the time constants of slow components in all the cell types were similar, the time constant of the fast component in cells with  $\beta_{2a}$  subunits was larger than those in cells with  $\beta_{2c}$  subunits and native cells. The proportion of the fast component was smaller and the proportion of the slow component was larger in cells with  $\beta_{2a}$  subunits than in cells with  $\beta_{2c}$  subunits and native cells. These findings suggest that the channel with the  $\beta_{2a}$  subunit favored the frequency of occupancy of long open state in comparison to the channel with the  $\beta_{2c}$  subunit and the native  $\text{Ca}^{2+}$  channel.

The open time histograms shown in Fig. 4 were constructed from selected low  $P_o$  mode (Fig. 4A–C) or high  $P_o$  mode (Fig. 4D–F) sweeps of all examined cells for each

experimental condition. These histograms were also fitted by two exponential functions. Table 1 shows the parameters for the open time components from each cell. The time constants of open time distributions of the high  $P_o$  mode were slower than those of the low  $P_o$  mode. This is a natural result considering that the high  $P_o$  mode mainly contained long-lasting openings. Within each mode, the parameters of open time distributions in cells with  $\beta_{2a}$  subunits, cells with  $\beta_{2c}$  subunits, and native cells were similar. As shown in Fig. 3, the occurrence of high  $P_o$  mode in cells with  $\beta_{2a}$  subunits was more frequent than that in cells with  $\beta_{2c}$  subunits and the native cells. This difference in the ratios of high  $P_o$  mode contributed to the difference in open time distributions of all sweeps.

### 3.4. Closed time distributions

The closed time distributions were analyzed similarly to the open time distributions. Table 2 shows the time constants and proportions of closed time components derived from each cell for statistical analysis. The closed time histograms could be fitted to the sum of three exponential functions in all cases. As can be seen in Table 2, the proportion of the slow closed time component of cells with  $\beta_{2a}$  subunits was smaller than those of cells with  $\beta_{2c}$  subunits and native cells. In Fig. 5, closed time histograms have been separated into high  $P_o$  sweeps and low  $P_o$  sweeps. The proportion of the slow component in the high  $P_o$  mode of the cells with  $\beta_{2a}$  subunits was smaller than those in other cells, but other parameters were indistinguishable between cells with  $\beta_{2a}$  subunits, cells with  $\beta_{2c}$  subunits, and native cells, as shown in Table 2. As shown in Fig. 3, sweeps showing very high  $P_o$  were much more frequent in cells with  $\beta_{2a}$  subunit than in cells with  $\beta_{2c}$  subunits and native cells. These observations indicate that the occurrence of long-lasting closings was

Table 2  
Time constants and proportions of closed time distributions

	Fast component		Middle component		Slow component	
	Time constant (ms)	Proportion	Time constant (ms)	Proportion	Time constant (ms)	Proportion
<i>All sweeps</i>						
$\beta_{2a}$	$2.17 \pm 0.30$	$0.81 \pm 0.03$	$16.05 \pm 5.22$	$0.16 \pm 0.03$	$169.82 \pm 41.01$	$0.04 \pm 0.02$
$\beta_{2c}$	$3.11 \pm 0.19$	$0.53 \pm 0.08$	$21.87 \pm 2.18$	$0.21 \pm 0.07$	$226.58 \pm 15.26$	$0.13 \pm 0.02^*$
Native	$2.76 \pm 0.37$	$0.71 \pm 0.06$	$22.09 \pm 2.24$	$0.12 \pm 0.01$	$209.10 \pm 18.52$	$0.11 \pm 0.01^*$
<i>Low <math>P_o</math> sweeps (mode 1)</i>						
$\beta_{2a}$	$3.55 \pm 0.65$	$0.68 \pm 0.10$	$29.57 \pm 10.38$	$0.17 \pm 0.06$	$226.55 \pm 16.34$	$0.13 \pm 0.01$
$\beta_{2c}$	$3.56 \pm 0.29$	$0.47 \pm 0.08$	$22.67 \pm 3.04$	$0.21 \pm 0.06$	$231.71 \pm 14.75$	$0.14 \pm 0.02$
Native	$2.99 \pm 0.43$	$0.67 \pm 0.08$	$22.83 \pm 3.22$	$0.12 \pm 0.11$	$218.62 \pm 21.28$	$0.12 \pm 0.01$
<i>High <math>P_o</math> sweeps (mode 2)</i>						
$\beta_{2a}$	$1.98 \pm 0.33$	$0.89 \pm 0.02$	$16.57 \pm 2.75$	$0.11 \pm 0.03$	$139.20 \pm 31.80$	$0.01 \pm 0.01$
$\beta_{2c}$	$2.26 \pm 0.24$	$0.71 \pm 0.08$	$26.30 \pm 5.61$	$0.12 \pm 0.04$	$118.16 \pm 7.58$	$0.08 \pm 0.02^*$
Native	$2.02 \pm 0.07$	$0.82 \pm 0.07$	$43.53 \pm 17.12$	$0.09 \pm 0.01$	$113.15 \pm 2.62$	$0.07 \pm 0.01^*$

Values are means  $\pm$  S.E.M. Three, four and five experiments were carried out for cells with  $\beta_{2a}$  subunits, cells with  $\beta_{2c}$  subunits, and native cells, respectively. Low  $P_o$  sweeps (mode 1),  $0 < \text{open probability} \leq 0.25$ ; high  $P_o$  sweeps (mode 2), open probability  $> 0.25$ .

\*Significant vs.  $\beta_{2a}$  group ( $P < 0.05$ ).

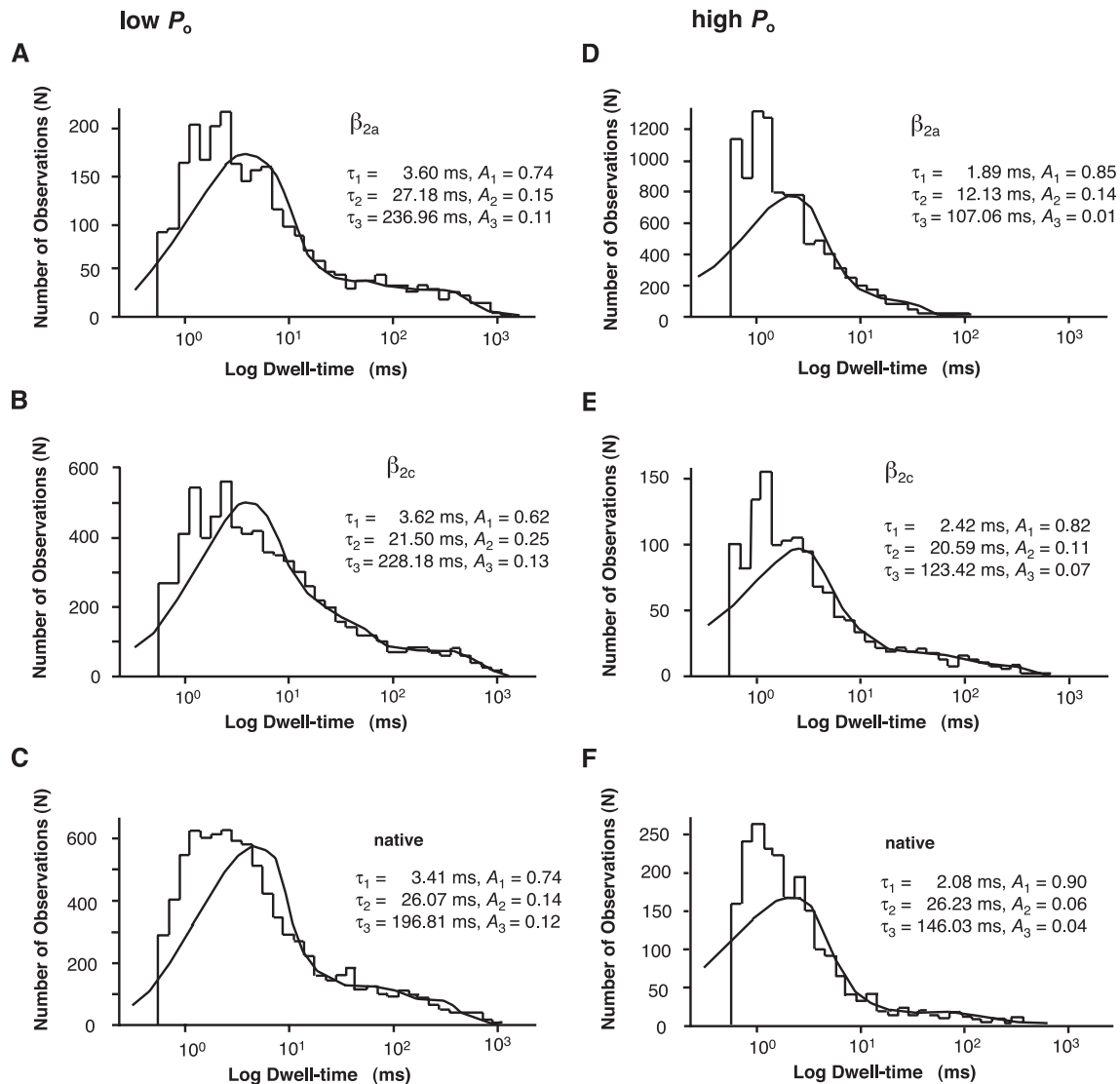


Fig. 5. Closed time histograms compiled from separated low  $P_o$  sweeps (A, B, C) and high  $P_o$  sweeps (D, E, F). The upper panel (A, D) shows histograms from cells with  $\beta_{2a}$  subunits, the middle panel (B, E) shows histograms from cells with  $\beta_{2c}$  subunits, and the lower panel (C, F) shows histograms from native cells.

much less frequent in cells with  $\beta_{2a}$  subunits than in other cells even in high  $P_o$  modes. The difference in the closed time histograms from all sweeps was due to the difference in the ratios of observed high  $P_o$  sweeps in each cell. In cells with  $\beta_{2a}$  subunits, the large fraction of high  $P_o$  mode reduced the proportion of the third component of closed time histograms from all sweeps.

#### 4. Discussion

Single-channel behavior of the  $\text{Ca}^{2+}$  channel with  $\beta_{2a}$  subunit was different from that of the channel with  $\beta_{2c}$  subunit. As the whole-cell current recorded from the cells transfected with  $\beta_{2c}$  subunits inactivated faster than that recorded from the cells transfected with  $\beta_{2a}$  subunits in our previous study (Yamada et al., 2001), ensemble-averaged

current of the cells with  $\beta_{2c}$  subunits declined fast, but that of the cells with  $\beta_{2a}$  subunits did not decline like that.

L-type  $\text{Ca}^{2+}$  channels show unique gating behavior, which includes three distinct forms of behavior, mode 0, mode 1, and mode 2 (Hess et al., 1984). Mode 0 refers to null sweeps, and the channels are unavailable for opening in this mode. Mode 1 is characterized by conventional brief openings, and  $P_o$  in this mode is relatively low. Mode 2 is distinguished by long-lasting openings, and  $P_o$  in this mode is relatively high. Because the levels of single-channel activities were too low, we used 1  $\mu\text{M}$  of Bay K 8644 in a pipette solution in the latter half of experiments. It is well known that Bay K 8644 facilitates the occurrence of mode 2 behavior (Hess et al., 1984). Concerning inactivation of ensemble-averaged current, the result of experiments with Bay K 8644 had similar tendency as that of experiments without Bay K 8644. It has been well known that Bay K

8644 binds to the DHP binding sites in IIS5, IIS6, and IVS6 of  $\alpha_{1c}$  subunit (Hofmann et al., 1999).

The percentage of sweeps in the high  $P_o$  ( $>0.25$ ) mode was larger in the cells with  $\beta_{2a}$  subunits than in the cells with  $\beta_{2c}$  subunits and the native cells. Within each mode, the open and closed time distributions in all three cell types were very similar. The difference in the ratios of occurrence of high  $P_o$  mode behavior contributed to the difference in open and closed time distributions as a whole. Anyway, as experiments were performed under the same conditions, it is certain that the properties of the native channels are comparable with those of the channels with  $\beta_{2c}$  subunit and different from those of the channels with  $\beta_{2a}$  subunit.

Although mode 1 gating predominates in the physiological conditions, it has been reported that mode 2 gating can be seen occasionally in the absence of Bay K 8644 (Pietrobon and Hess, 1990). It is reported that mode 2 gating is enhanced by  $\beta$ -adrenergic stimulation like Bay K 8644 (Yue et al., 1990). It has also been reported that mode 2 gating frequently occurs in early stage of development of embryonic chick (Tohse et al., 1992) and rat (Masuda et al., 1995) heart cells. It seems to be significant that the occurrence of mode 2 gating behavior varies depending on the type of  $\beta$  subunit under physiological conditions.

On the other hand, it has been reported that the  $\beta_{2a}$  subunit alters the modal gating behavior of the cardiac  $\text{Ca}^{2+}$  channels without creating any new open state in the presence of 10  $\mu\text{M}$  of Bay K 8644 (Costantin et al., 1998). It is also possible that the  $\beta$  subunit of the L-type  $\text{Ca}^{2+}$  channel affects its modal gating behavior. The  $\beta_{2a}$  subunit might act differently from the  $\beta_{2c}$  subunit on the modal gating behavior of the  $\text{Ca}^{2+}$  channels.

The  $\beta$  subunit did not change the unit amplitude of  $I_{\text{Ba}}$  of  $\text{Ca}^{2+}$  channels in the present study. The slope conductances of  $\text{Ca}^{2+}$  channels in the cells with  $\beta_{2a}$  subunits, the cells with  $\beta_{2c}$  subunits, and the native cells were identical.

Until recently, the  $\beta_{2a}$  subunit was the only  $\beta_2$  splice variant described in the rat heart (Perez-Reyes et al., 1992). In the present study, the single-channel property of  $\text{Ca}^{2+}$  channels reconstituted with  $\beta_{2a}$  subunits was found to be different from that of native channels. This result agrees with the results of our present study (Yamada et al., 2001) and other previous studies (Qin et al., 1998; Wei et al., 2002) cast doubt on the functional roles of the  $\beta_{2a}$  subunit in cardiac myocytes. We could not conclude that the  $\beta_{2a}$  subunit is not expressed in the heart, but it seems probable that the  $\beta_{2a}$  subunit is not a major  $\beta_2$  subunit expressed in the heart.

We previously cloned the  $\beta_{2c}$  subunit from the rat heart (Yamada et al., 2001). We detected abundant expression of mRNA of the  $\beta_{2c}$  subunit but failed to detect mRNA of the  $\beta_{2a}$  subunit in the rat heart. Whole-cell patch clamp recordings showed that the inactivation kinetics of recombinant  $\text{Ca}^{2+}$  currents of the cells with  $\beta_{2c}$  subunits were different from those of the cells with  $\beta_{2a}$  subunits but comparable with those of the native cells. Taken together with these

previous results, the results of single-channel analysis suggest that the  $\beta_{2c}$  subunit is one of the functional  $\beta_2$  subunits expressed in the heart. However, we could not reconstitute the native  $\text{Ca}^{2+}$  channel completely, although we used  $\alpha_{1c}$ ,  $\beta_{2c}$  and  $\alpha_2\delta$  subunits, which were cloned from the rat heart. In our previous study, the sustained components of  $I_{\text{Ba}}$  recorded from native cardiac myocytes were significantly greater than those from the cells with  $\beta_{2c}$  subunit (Yamada et al., 2001). In the present study, while the ensemble average current of the  $\beta_{2c}$  channels was almost zero at pulse end, there was residual component at pulse end of native channels. The possibility that other  $\beta$  subunits and/or other unknown regulators also function in cardiac myocytes cannot be ruled out. The activities of modulators of the  $\text{Ca}^{2+}$  channel, such as calmodulin (Peterson et al., 1999), in native cardiac myocytes might be different from those in heterologous expression systems. Recently, it was reported that a novel splice variant of the  $\beta_2$  subunit ( $\beta_{2b}$  subunit) is cloned from the rat heart and the gating property of channels in heart cells transfected with the  $\beta_{2b}$  subunit is virtually identical to that of native unmodified channels (Colecraft et al., 2002). Although it is not clear whether there is heterogeneity of  $\beta$  subunits in cardiac myocytes, the  $\beta_{2c}$  subunit might be one of the  $\beta$  subunits of the heart, and the  $\beta_{2b}$  subunit might be also functional.

In summary, single-channel properties of recombinant  $\text{Ca}^{2+}$  channels using  $\beta_{2c}$  subunits resembled those of native cardiac  $\text{Ca}^{2+}$  channels and were different from those of recombinant  $\text{Ca}^{2+}$  channels with  $\beta_{2a}$  subunits. The  $\beta$  subunit affected the modal gating behavior of the  $\text{Ca}^{2+}$  channels. These results combined with the results of our previous study suggest that the  $\beta_{2c}$  subunit is one of the functional  $\beta_2$  subunits expressed in the heart.

## References

- Bers, D.M., 2002. Cardiac excitation–contraction coupling. *Nature* 415, 198–205.
- Birnbaumer, L., Qin, N., Olcese, R., Tareilus, E., Platano, D., Costantin, J., Stefani, E., 1998. Structures and functions of calcium channel  $\beta$  subunits. *J. Bioenerg. Biomembranes* 30, 357–375.
- Catterall, W.A., 2000. Structure and regulation of voltage-gated  $\text{Ca}^{2+}$  channels. *Annu. Rev. Cell Dev. Biol.* 16, 521–555.
- Colecraft, H.M., Alseikhan, B., Takahashi, S.X., Chaudhuri, D., Mittman, S., Yegnashubramanian, V., Alvania, R.S., Johns, D.C., Marban, E., Yue, D.T., 2002. Novel functional properties of  $\text{Ca}^{2+}$  channel  $\beta$  subunits revealed by their expression in adult rat heart cells. *J. Physiol.* 541, 435–452.
- Costantin, J., Noceti, F., Qin, N., Wei, X., Birnbaumer, L., Stefani, E., 1998. Facilitation by the  $\beta_{2a}$  subunit of pore openings in cardiac  $\text{Ca}^{2+}$  channels. *J. Physiol.* 507, 93–103.
- Hess, P., Lansman, J.B., Tsien, R.W., 1984. Different modes of Ca channel gating behaviour favoured by dihydropyridine Ca agonists and antagonists. *Nature* 311, 538–544.
- Hofmann, F., Biel, M., Flockerzi, V., 1994. Molecular basis for  $\text{Ca}^{2+}$  channel diversity. *Annu. Rev. Neurosci.* 17, 399–418.
- Hofmann, F., Lacinova, L., Klugbauer, N., 1999. Voltage-dependent calcium channels: from structure to function. *Rev. Physiol., Biochem. Pharmacol.* 139, 35–87.

- Isenberg, G., Klockner, U., 1982. Calcium tolerant ventricular myocytes prepared by preincubation in a “KB medium”. *Pflügers Arch.* 395, 6–18.
- Lacerda, A.E., Kim, H.S., Ruth, P., Perez-Reyes, E., Flockerzi, V., Hofmann, F., Birnbaumer, L., Brown, A.M., 1991. Normalization of current kinetics by interaction between the  $\alpha_1$  and  $\beta$  subunits of the skeletal muscle dihydropyridine-sensitive  $\text{Ca}^{2+}$  channel. *Nature* 352, 527–530.
- Masuda, H., Sumii, K., Sperelakis, N., 1995. Long openings of calcium channels in fetal rat ventricular cardiomyocytes. *Pflügers Arch.* 429, 595–597.
- Perez-Reyes, E., Schneider, T., 1995. Molecular biology of calcium channels. *Kidney Int.* 48, 1111–1124.
- Perez-Reyes, E., Castellano, A., Kim, H.S., Bertrand, P., Bagstrom, E., Lacerda, A.E., Wei, X.Y., Birnbaumer, L., 1992. Cloning and expression of a cardiac/brain  $\beta$  subunit of the L-type calcium channel. *J. Biol. Chem.* 267, 1792–1797.
- Peterson, B.Z., DeMaria, C.D., Adelman, J.P., Yue, D.T., 1999. Calmodulin is the  $\text{Ca}^{2+}$  sensor for  $\text{Ca}^{2+}$ -dependent inactivation of L-type calcium channels. *Neuron* 22, 549–558.
- Pietrobon, D., Hess, P., 1990. Novel mechanism of voltage-dependent gating in L-type calcium channels. *Nature* 346, 651–655.
- Qin, N., Platano, D., Olcese, R., Costantin, J.L., Stefani, E., Birnbaumer, L., 1998. Unique regulatory properties of the type 2a  $\text{Ca}^{2+}$  channel  $\beta$  subunit caused by palmitoylation. *Proc. Natl. Acad. Sci. U. S. A.* 95, 4690–4695.
- Tohse, N., 1990. Calcium-sensitive delayed rectifier potassium current in guinea pig ventricular cells. *Am. J. Physiol.* 258, H1200–H1207.
- Tohse, N., Meszaros, J., Sperelakis, N., 1992. Developmental changes in long-opening behavior of L-type  $\text{Ca}^{2+}$  channels in embryonic chick heart cells. *Circ. Res.* 71, 376–384.
- Wei, S.K., Colecraft, H.M., DeMaria, C.D., Peterson, B.Z., Zhang, R., Kohout, T.A., Rogers, T.B., Yue, D.T., 2002.  $\text{Ca}^{2+}$  channel modulation by recombinant auxiliary  $\beta$  subunits expressed in young adult heart cells. *Circ. Res.* 86, 175–184.
- Yamada, Y., Nagashima, M., Tsutsuura, M., Kobayashi, T., Seki, S., Makita, N., Horio, Y., Tohse, N., 2001. Cloning of a functional splice variant of L-type calcium channel  $\beta_2$  subunit from rat heart. *J. Biol. Chem.* 276, 47163–47170.
- Yue, D.T., Herzig, S., Marban, E., 1990.  $\beta$ -Adrenergic stimulation of calcium channels occurs by potentiation of high-activity gating modes. *Proc. Natl. Acad. Sci. U. S. A.* 87, 753–757.